Spectral-reflectance reconstruction in the near-infrared region by use of conventional charge-coupled-device camera measurements

Meritxell Vilaseca, Jaume Pujol, and Montserrat Arjona

Our aim is to develop a method for obtaining the reflectance spectra of samples in the near-infrared (NIR) region (800–1000 nm) by using a small number of measurements performed with a conventional CCD camera (multispectral imaging). We experimentally determined the spectral sensitivity of the CCD camera in the NIR range, used a method based on principal component analysis to reconstruct the spectral reflectance of the samples, and analyzed the number and shape of the filters that need to be used to apply this method. Finally we obtained the reflectance spectra of a set of 30 spectral curves by numerical simulation. The small amount of errors in the spectral reconstruction shows the potential of this method for reconstructing spectral reflectances in the NIR range. © 2003 Optical Society of America

OCIS codes: 040.1520, 110.3080, 120.6200, 150.3040.

1. Introduction

The use of solid-state detector arrays[1,2] has increased rapidly in the past few years, specifically in the case of video cameras, owing to their versatility and low cost. They employ a solid-state array that allows the conversion of light into measurable voltage signals. The detector can be based on various technologies, such as the CCD, the complementary metal-oxide semiconductor, or the charge injection device. The advantages of some of these devices permit their use in several applications.

The spectral response of conventional CCD cameras extends from the visible to the near infrared (NIR). In general, it is clearly significant to as great as 1000 nm. CCD cameras with improved response in the NIR region are currently being manufactured. Therefore we can use this standard and simple instrumentation in NIR applications, using its response in this specific range. Meanwhile the visible spectrum contains very little information on the chemical composition of an object; the spectral information included in the NIR region (800–1000 nm) is in general directly related to the constituents of a material. In the NIR spectrum there are absorption peaks corresponding to specific vibrations of molecules present in the material so that they can be identified. Therefore it is used as an analytical tool in industry and research, known as NIR technology.[3] NIR technology is used in a vast number of applications. They include agriculture, the food industry, clinical diagnostics, pharmaceutical production, and the chemical and petrochemical industry.

The photon-flux incident on an IR sensor imaging system can have both reflected and thermally self-emitted components. In the NIR region the dominant mechanism is reflected photons. Therefore the limitation of thermal IR imaging systems related to poor contrast between objects and backgrounds can be overcome. Also the proximity of the NIR to the visible region permits the application of color-vision methods in this range.[4,5] A drawback of working only in the NIR region can be the spectral reflectivity of objects not having enough variability.

To obtain the reflectance spectra of samples by using measurements performed with any optoelectronic sensor as a CCD camera, it is necessary to know its spectral sensitivity. The methods of spectral characterization used to determine the sensitivity of optoelectronic devices can be classified into two groups.

The authors are with Departament d'Òptica i Optometria, Centre de Desenvolupament de Sensors, Instrumentació i Sistemes (CD6), Universitat Politècnica de Catalunya, Rambla Sant Nebridi 10, 08222 Terrassa, Spain. M. Vilaseca's e-mail address is mvilasec@oo.upc.es.

Received 26 April 2002; revised manuscript received 15 October 2002.

0003-6935/03/101788-10$15.00/0

The first class of methods[6–10] is based on direct spectral measurements and use of optoelectronic conversion spectral functions (OECSFs) to obtain spectral sensitivity. These functions relate the camera responses (normalized output *NO*) with the incident exposure *H* for each wavelength. To apply this class of methods, it is necessary to use a device that emits monochromatic light and a radiometer that finds the exposure level for each measurement. The second class of methods[11–13] involves estimating the spectral sensitivity relating the camera responses for certain samples to their known reflectance or transmittance spectra. If X_i is a column vector of i rows and its components are the camera responses of different samples and R is a matrix of i rows where each row is the spectral reflectance of a sample at j wavelengths, we can write $X_i = RS_\lambda$. The method therefore consists of resolving this equation and determining vector S_λ (j rows), which represents the estimated spectral sensitivity of the camera. The difficulty with this method is choosing which samples to use in resolving the equation, since the estimated sensitivity may change. Although methods based on direct spectral measurements are more complicated and elaborate, the results are more reliable than with the second class of methods, since no estimation is made.

If the spectral sensitivity of the camera and the spectral radiance of the illuminant used are known, it is possible to estimate the spectral reflectance of samples by using measurements of different spectral bands of the CCD camera (multispectral imaging). The different spectral bands can be obtained by placing a set of carefully selected optical filters in front of the camera. With a simple configuration we can use these conventional and relatively inexpensive devices instead of the standard spectrophotometers currently used in NIR technology. Spectrophotometric instruments are expensive, since they normally use a diffraction grating to obtain monochromatic light. There are different methods for reconstructing spectral data, some of them based on interpolation calculations (linear, cubic, spline, discrete Fourier transform, and modified discrete sine transform approximations) and others on estimation or fitting techniques (the Moore–Penrose pseudoinverse, the smoothing inverse, the Wiener inverse, nonlinear fittings, and the principal component analysis or characteristic vector analysis[14–17]). In this study we use the principal component analysis (PCA) method to reconstruct the spectral reflectance of the analyzed samples. With this technique a number of sets of spectral curves are inspected and basis curves called characteristic vectors are determined. A small quantity of characteristic vectors combined in the proper amounts is capable of describing or reconstructing each of the original spectral curves or similar spectra. As a result any spectral reflectance curve can be represented by a small number of vectors that contain essentially all the information of the original data. Other methods of reconstruction[18–20] are based on relating the spectral reflectances of samples with the corresponding camera responses by using an estimated matrix. Such methods fix this matrix, decreasing the Euclidian distance between the original reflectance spectra and the reconstructed spectra, or equivalently decreasing the Euclidian distance between the real camera response and the estimated response for a given reflectance spectra.

To recover spectral reflectances by using multispectral images, it is necessary to incorporate a set of filters in the CCD camera. Many authors[21–27] have studied the influence of these filters in the visible region, since they constitute a basic component of many color-reproduction systems.

To obtain a good color-scanning process, the responses of the spectral bands of the camera need to be a linear combination of the color-matching functions of the CIE-1931 XYZ standard observer. In the NIR the election of the filters is conditioned by the amount of reconstruction of the spectral curves, because no colorimetric space is defined in the studied region, and we use simple transmittance profiles to obtain available commercial filters.

In this study we present an experimental technique for obtaining the spectral sensitivity of a CCD camera in the NIR region by using a method based on direct spectral measurements. We use a PCA-based method for reconstructing spectral reflectance curves of samples in the 800–1000-nm range. This method uses measurements performed with a conventional CCD camera. In Section 3 we analyze the number and shape of the filters to be used in various channels to obtain good reconstructions in the NIR region. We use simple transmittance profiles to obtain available commercial filters. Using numerical simulation, we analyzed the results of reconstruction that would be obtained for spectral curves with different sets of filters, under the influence of two different illuminants. Finally we also compare the PCA-obtained results with other existing reconstruction methods. To date, no spectral reconstruction methods in the NIR region when conventional CCD camera measurements are used have been reported.

2. Method

A. Spectral Characterization

The experimental setup used to perform the spectral characterization of an optoelectronic capture device, normally composed of a solid-state camera, the optics, and a frame grabber, is shown in Fig. 1. The CCD camera provides the greatest contribution to overall spectral sensitivity, since the response of the frame grabber has no spectral dependency and the optics have only little wavelength variability. Our image-capture device consisted of a progressive scan camera JAI CV-M10 with a commercial Vivitar lens (70–120 mm) connected to a Matrox IP8 frame grabber on a PC. The digital response of the camera for a uniform and monochromatic image obtained with a diffuser was measured for the 800–1000-nm wavelength range in 10-nm steps. The target radiance was varied by using the entrance/exit slits of a

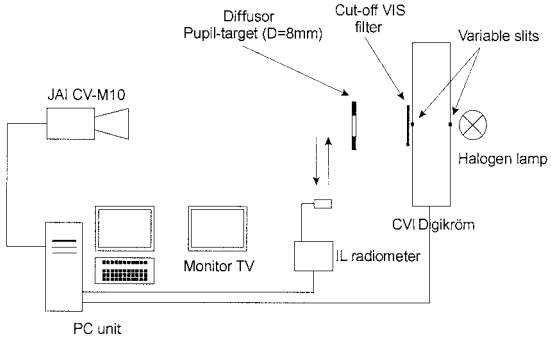

Fig. 1. Experimental setup for spectral characterization.

CVI Laser Digikröm monochromator with constant spectral resolution attached to a conventional halogen lamp. The target radiance was measured with an International Light IL-1700 radiometer. We put a visible cutoff filter in front of the monochromator to ensure that the radiance of the image was composed only of radiation coming from the NIR region. We configured the gain of the camera and the gain and offset of the frame grabber for a linear response to the radiance. The integration time used was $t = 20$ ms.

In the spectral characterization method applied the spectral sensitivity is derived from the OECSF. These functions relate the camera response to the exposure level for each wavelength:

$$NO_\lambda = H_\lambda\left[\frac{1}{(2^{\text{bit}} - 1)}\frac{\lambda}{hc}\frac{\eta_\lambda}{K_\lambda}\right], \tag{1}$$

where NO_λ is the spectral normalized output, H_λ is the spectral exposure, η_λ is the spectral quantum efficiency, and K_λ is the inverse of the optoelectronic conversion constant obtained with the photon-transfer technique.[1]

The exposure can be calculated from the radiance as follows:

$$H_\lambda = \frac{\pi}{4}\frac{A_{\text{sensor}}}{(1 + m_{\text{obj}})^2}\frac{L_{e\lambda}}{F^2}\tau_{\text{obj}}T_{\text{atm}}t, \tag{2}$$

where A_{sensor} is the irradiated sensor area, $L_{e\lambda}$ is the incident spectral radiance, τ_{obj} is the spectral transmittance of the objective lens, T_{atm} is the spectral transmittance of the atmosphere, t is the integration time, m_{obj} is the lateral magnification of the objective lens of the camera, and F is the f-number of the objective lens.

In our experiment the spectral exposure was given by

$$H_\lambda = 1.60578 \times 10^{-8}L_{e\lambda}(\text{J}), \tag{3}$$

where an f-number, $F = 4.5$, is used.

The experimental OECSF of a camera can be fitted mathematically by sigmoid functions[28] with four parameters defined as

$$NO_\lambda = a_\lambda + \frac{b_\lambda}{1 + \exp\left[-\dfrac{(H_\lambda - c_\lambda)}{d_\lambda}\right]}. \tag{4}$$

From these functions it is possible to calculate two equivalent magnitudes that may be derived from the general concept of spectral sensitivity: spectral responsivity $r(\lambda, H_\lambda)$, defined as the response to a spectral stimulus with constant energy, and action spectrum $a(\lambda, NO_\lambda)$, defined as the inverse of the energy of spectral stimuli that give a constant response:

$$r(\lambda, H_\lambda) = \frac{\text{response}}{\text{constant energy}},$$

$$r(\lambda, H_\lambda) = \frac{a_\lambda + \dfrac{b_\lambda}{1 + \exp\left[-\dfrac{(H_\lambda - c_\lambda)}{d_\lambda}\right]}}{H_\lambda}. \tag{5}$$

$$a(\lambda, NO_\lambda) = \frac{\text{constant response}}{\text{energy}},$$

$$a(\lambda, NO_\lambda) = \frac{NO_\lambda}{c_\lambda - d_\lambda \ln\left[\dfrac{b_\lambda}{(NO_\lambda - a_\lambda)} - 1\right]}. \tag{6}$$

Both functions represent the (NO_λ/H_λ) ratio, but the spectral responsivity is a function of the wavelength and the exposition H_λ, while the action spectrum is a function of the wavelength and the normalized output NO_λ. The spectral sensitivity of the CCD camera can be calculated indistinctly from the relative scaling of one of these magnitudes versus the wavelength for different constant exposures (spectral responsivity) or normalized outputs (action spectrum).

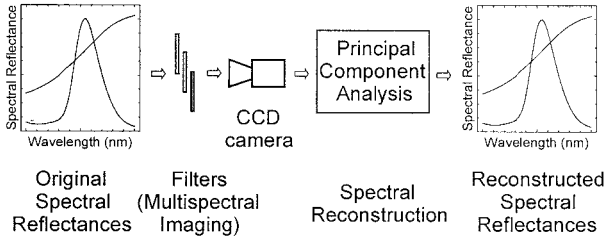

Fig. 2. Complete chain of the multichannel image-acquisition system and the final spectral-reconstruction step.

B. Spectral Reconstruction

The reconstruction method used is summarized in Fig. 2. A multichannel image of an original object is acquired by placing a selected set of filters in front of the camera. To recover the spectral-reflectance curves of different samples, we use a method based on PCA.[14] To use this method, it is necessary to know the sets of spectral reflectance data similar to the

curves that we want to reconstruct. Each spectral curve is interpreted as a vector of n components. The set of m known spectral-reflectance curves is represented by an $m \times n$ matrix called the original data matrix. This matrix can be associated with a vector space, and its characteristic vectors can be calculated. By using the whole set of characteristic vectors, it is possible to recover the original vector space in its totality. Specifically, to reconstruct each of the original curves $\mathbf{z}$, each calculated characteristic vector must be added in the proper amount (linear combination) to the mean curve or vector $\mathbf{z}_M$ (which represents the average of the original m curves). In vector notation this can be stated as

$$\mathbf{z} \cong \mathbf{z}_M + \alpha\mathbf{v}_1 + \beta\mathbf{v}_2 + \gamma\mathbf{v}_3 + \delta\mathbf{v}_4 + \cdots + \xi\mathbf{v}_p, \quad p \leq n, \tag{7}$$

where $\alpha, \beta, \ldots, \xi$ are scalar coefficients and $\mathbf{v}_1, \mathbf{v}_2, \ldots, \mathbf{v}_p$ are the characteristic vectors.

The scalar coefficients are the amounts of the characteristic vectors that must be combined to recover each spectral curve. To explain the differences along all the spectral curves (each represented by n values), it is necessary to equate p to n because of the vector-space definition. It is demonstrated that a small set of characteristic vectors can explain a large percentage of variability of the original and other similar curves, and for this reason from now on we consider that $p < n$.

The CCD camera responses for each channel can be expressed as

$$X_i = \int_{\lambda_{\min}}^{\lambda_{\max}} i(\lambda) r(\lambda) \tau(\lambda) F_i(\lambda) S(\lambda) \mathrm{d}\lambda, \tag{8}$$

where X_i is the digital level obtained for a certain channel, $i(\lambda)$ is the spectral radiance of the illuminant, $r(\lambda)$ is the spectral reflectance of the sample, $\tau(\lambda)$ is the spectral transmittance of the optical path, $F_i(\lambda)$ is the spectral transmittance of the filters placed between the camera and the sample (different for each channel), and $S(\lambda)$ is the spectral sensitivity of the CCD camera used. The term $\tau(\lambda)$ includes the optical system in front of the camera (objective lens) as well as the spectral transmittance of the atmosphere. We consider the value of this term 1, which is approximately its value in normal conditions.

The spectral radiance of the illuminant, the spectral reflectance of the sample, and the spectral sensitivity of the camera can be brought together in a term called $R(\lambda)$:

$$R(\lambda) = i(\lambda) r(\lambda) S(\lambda). \tag{9}$$

We can write Eq. (8) as

$$X_i = \int_{\lambda_{\min}}^{\lambda_{\max}} R(\lambda) F_i(\lambda) \mathrm{d}\lambda \tag{10}$$

for each existing channel of the camera.

In vector notation

$$X_i = \mathbf{R}\mathbf{F}_i. \tag{11}$$

This association is useful because the filters remain separate from the rest of the variables, although other types of association provide similar results. If we consider the spectral curves to be reconstructed as $\mathbf{R}$ vectors and we have an original data matrix containing similar curves, we can write expression (7) as

$$\mathbf{R} \approx \mathbf{R}_M + \alpha\mathbf{v}_1 + \beta\mathbf{v}_2 + \gamma\mathbf{v}_3 + \ldots + \xi\mathbf{v}_p, \qquad p < n, \tag{12}$$

where $\mathbf{v}_1, \mathbf{v}_2, \ldots, \mathbf{v}_p$ are the characteristic vectors of the original data matrix used and $\mathbf{R}_M$ is the mean vector of the original data matrix.

In fact the response of the camera X_i will be known and $\mathbf{R}$ will be the unknown spectrum that we wish to reconstruct from the camera measurements. By combining Eq. (11) and expression (12), we can write

$$X_i = \mathbf{R}\mathbf{F}_i \approx \mathbf{R}_M\mathbf{F}_i + \alpha\mathbf{v}_1\mathbf{F}_i + \beta\mathbf{v}_2\mathbf{F}_i + \gamma\mathbf{v}_3\mathbf{F}_i + \ldots + \xi\mathbf{v}_p\mathbf{F}_i, \qquad p < n. \tag{13}$$

Equation (13) relates the camera responses for each channel to the reconstruction parameters. We know all the variables of Eq. (13) except the scalar coefficients $\alpha, \beta, \ldots, \xi$. We have the same number of scalar coefficients as characteristic vectors that we want to use in the reconstruction. To find the value of these coefficients, the same number of equations as unknown quantities is needed (the same number of channels or filters as characteristic vectors used in the reconstruction). After these coefficients are calculated we can apply expression (12) to reconstruct $\mathbf{R}$, and consequently we can determine the spectrum of the unknown sample. $\mathbf{R}$ is not the isolated reflectance spectrum of the sample but includes the spectral radiance of the illuminant used and the spectral sensitivity of the CCD camera. Therefore, to obtain the spectral reflectance of the sample, we must extract the influence of the illuminant as well as the spectral sensitivity of the camera, dividing each component $R(\lambda)$ of the curve reconstructed by term $S(\lambda)i(\lambda)$. Furthermore, to apply the proposed reconstruction method, we use an original data matrix composed of spectral $\mathbf{R}$ curves. This means that these curves incorporate the illuminant used. The calculated characteristic vectors are therefore for a particular illuminant. If we want to apply the method for many illuminants, we must know the original data matrix under the influence of every type of illuminant. We are then able to calculate the characteristic vectors without introducing errors.

To evaluate the quality of the reconstruction, we use two different parameters:

percentage of reconstruction,

$$P_{\mathrm{rec}} = \left[1 - \frac{\sum_{\lambda_{\min}}^{\lambda_{\max}} (r_{\mathrm{exp}} - r_{\mathrm{rec}})^2}{\sum_{\lambda_{\min}}^{\lambda_{\max}} (r_{\mathrm{exp}})^2} \right] \times 100, \quad (14)$$

and root-mean-square error,

$$RMSE = \left[\frac{1}{N_\lambda} \sum_{\lambda_{\min}}^{\lambda_{\max}} (r_{\mathrm{exp}} - r_{\mathrm{rec}})^2 \right]^{1/2}, \quad (15)$$

where r_{exp} are the experimental components of the original reflectance curves, r_{rec} are the reconstructed values, and N_λ are the number of wavelengths where the measurements are made. *RMSE* is a commonly used parameter in multispectral imaging[15,16,18] and provides a nonlimited value related to the difference between the original and the reconstructed spectra. The percentage of reconstruction provides a more intuitive idea of the quality of the reconstruction since its maximum possible value is 100. However, the percentage of reconstruction parameter is sensitive to variations, and in some cases a percentage of 99% or less can lead to considerable differences between the original and the reconstructed spectra. Even a really bad reconstruction can lead to a negative percentage that is meaningless.

C. Filter Choice

The reconstruction of spectra explained above involves the use of various acquisition channels (different filters). The issue at hand is to decide which filters to use to obtain the best reconstruction in the NIR region. The reconstruction of spectral reflectance is performed with a limited number of characteristic vectors. The camera response for each channel is described by expression (13) but this is not an exact equality. It is a better or worse approximation depending on the number of vectors used, and this involves variations in the final scalar coefficients according to the filters used to resolve the equation. Therefore the quality of the spectral reconstruction may vary with the chosen filters, and the process can be optimized by performing a study to establish the set of filters that yields the best results.

There are many possible filter choices. The first option would be to use a set of heuristically chosen filters covering the NIR spectrum. The second would be to use filters with the same shape as the characteristic vectors, which would simplify the equations to be resolved. However, the components of the characteristic vectors can be negative, and they cannot be interpreted as transmittance of the filters. We can linearly transform these vectors in order to move their components into the interval (0, 1), but generally these filters are not easily manufactured because of their special profiles. To choose a set of easily available filters, we can choose equispaced Gaussian filters. We can use this type of filter to optimize the process. Also, to simplify the choice, we can fix some conditions beforehand. We consider that the filters used are filters with the following transmittance:

$$T(\lambda) = T_{\max} \exp\left[-0.5 \left(\frac{\lambda - \lambda_0}{\Delta\lambda} \right)^2 \right], \quad (16)$$

where $T_{\max}$ is the maximum height of the Gaussian peak, λ_0 is the wavelength corresponding to the maximum (center) of the Gaussian, and $\Delta\lambda$ is related to the FWHM of the Gaussian.

The ideal supposed maximum transmittance $T_{\max}$ is 1. In this case each channel has a different sensitivity. The results do not depend on the value of $T_{\max}$ because this parameter can be removed from the equations. Even though the results of the reconstruction are not modified, it can be useful to employ filters with a parameter $T_{\max}$ that provides channels with constant sensitivity.

The filters are considered equispaced in the 800–1000-nm region, and parameter λ_0 is therefore also fixed according to the number of filters used.

The parameter $\Delta\lambda$ is considered the optimization parameter. It is increased progressively in the same way for all the filters, and we choose the value that provides the best reconstruction for the spectral curves belonging to the original data matrix. We can modify parameter $\Delta\lambda$ independently for each filter, but this leads to high computational cost not justified by the results.

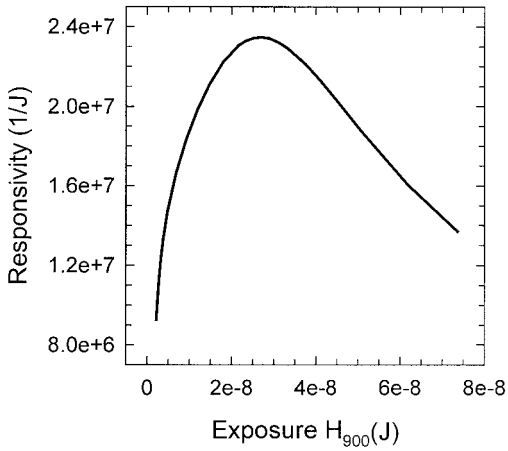

Fig. 3. Responsivity of the JAI CV-M10 camera corresponding to $\lambda = 900$ nm.

3. Results

Figures 3 and 4 show the responsivity and the action spectrum of the JAI CV-M10 camera for $\lambda = 900$ nm, obtained according to Eqs. (5) and (6). Figures 3 and 4 show the nonlinear behavior of the camera. Linear behavior implies a constant value of responsivity or action spectrum. The relative scaling of the spectral responsivity (action spectrum) remains nearly constant for different spectral profiles with different constant exposures (normalized outputs). Conse-

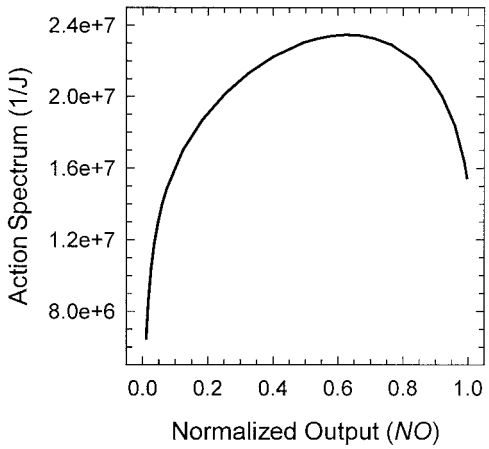

Fig. 4. Action spectrum of the JAI CV-M10 camera corresponding to $\lambda = 900$ nm.

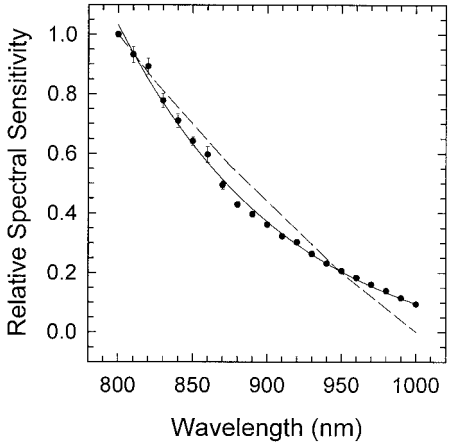

Fig. 6. Solid curve, dots, experimental relative spectral sensitivity of the JAI CV-M10 camera; dashed line, corresponding standard deviation and relative spectral sensitivity provided by the manufacturer.

quently we can characterize the spectral response of a camera in the NIR region by averaging the profiles of relative spectral responsivity (action spectrum) for different constant exposures (normalized outputs) (see Fig. 5). The relative spectral sensitivity obtained experimentally and that provided by the manufacturer are shown in Fig. 6. Although both profiles are similar, the curve provided by the manufacturer is more linear than that experimentally obtained. In general we find a lower spectral sensitivity in the whole region, except for the large wavelengths ($\lambda > 950$ nm) where a higher response is found.

To test the exposed method of spectral reconstruction and to estimate the results that we would obtain with it, we performed a simulation of the reconstructions for different samples. The original data matrix considered for the simulation consisted of 30 spectral curves (Fig. 7). Nineteen were real and 11 were theoretical or unreal curves. Compared with visible spectral reflectances, the NIR spectra of the samples are normally smooth and repetitive because of the sample's dependency on chemical composition.[3]

In the NIR region there are absorption peaks corresponding to specific vibrations of molecules in the material, but normally those peaks appear to overlap because of the radiation scatter and surface reflectance also present. However, we chose theoretical curves in order to obtain greater differences between the original curves and therefore to verify use of this method in worse-than-normal conditions. We considered the spectral data between 800 and 1000 nm in 10-nm steps. Therefore each curve was made up of 21 components. The simulated reconstructions were performed with a minimum of 2 and a maximum of 6 filters under the influence of two different halogen lamps with color temperatures, $Tc_1 = 2852$ K and $Tc_2 = 3371$ K. These two temperatures cover a wide real range, and the results can thus be applied in several lighting conditions. The spectral radiance of both illuminants is represented in Fig. 8. We can calculate the responses for each channel by using Eq. (11) because the spectral reflectance in the NIR re-

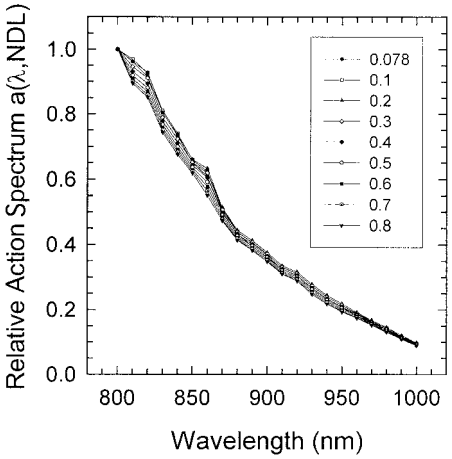

Fig. 5. Relative action spectrum corresponding to the following normalized outputs: 0.078, 0.1, 0.2, 0.3, 0.5, 0.6, 0.7, and 0.8.

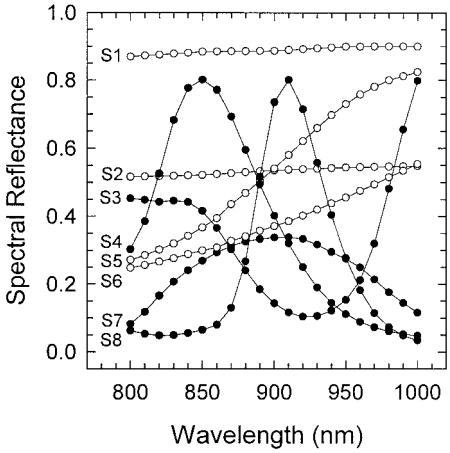

Fig. 7. Spectral reflectance curves of eight representative samples (S1, S2, S3, S4, S5, S6, S7, S8) belonging to the original data matrix: solid circles, theoretical curves; open circles, real curves).

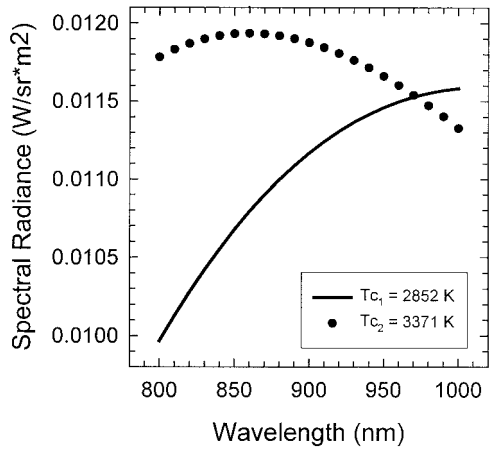

Fig. 8. Spectral radiance of the halogen lamps used in the simulation.

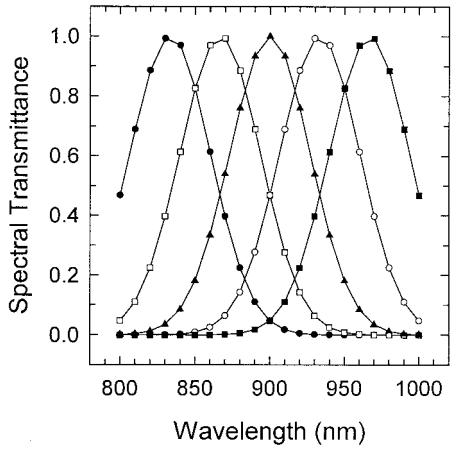

Fig. 9. Spectral transmittance of the five optimum filters obtained with the illuminant of color temperature, $Tc_1 = 2852$ K.

gion, the illuminant used, and the sensitivity of the camera are known. The optimization process was carried out by searching for the best reconstruction parameters (P_{rec} and *RMSE*) of all the curves belonging to the original data matrix.

The best reconstruction parameters obtained for all the performed simulations are indicated in Table 1. In Table 1 the optimum parameter $\Delta\lambda$ and the mean, standard deviation, maximum and minimum P_{rec}, and *RMSE* values for all the simulated cases are shown. It can be seen that the shape of the best filters (parameter $\Delta\lambda$) depends on the number of filters used in the simulation process. The transmittance of the five best obtained Gaussian filters ($\Delta\lambda = 27$) for the illuminant of color temperature, $Tc_1 = 2852$ K, is represented in Fig. 9. It can be seen that the optimum obtained filters have a large spectral width and are therefore easily commercially available. Figure 10 shows the spectral sensitivity for each of the five corresponding channels, taking into account the spectral response of the JAI CV-M10 camera, the emitted spectral radiance of the illuminant, and the transmittance of the corresponding filters.

As expected, the reconstructions improve with the use of more filters. The evolution of the reconstruction parameters with the number of filters is represented in Fig. 11. With two filters the reconstruction parameters (P_{rec} and *RMSE*) are bad, and both have a large standard deviation value of the associated results. With three and four filters the results improve but they still present high dispersion. With the use of five filters the percentage of reconstruction increases and there is little associated dispersion. Likewise *RMSE* decreases and has a low standard deviation value. Although the reconstructions improve further with the use of six filters, the changes are very small and the reconstruction parameters have almost constant values. With five filters the percentage of reconstruction is higher than 99.9% for each of the curves, and the (*RMSE**100) is smaller than 1, even when the theoretical and less smooth curves are considered. These values lead to an almost perfect reconstruction of the samples.

Table 1. Parameter $\Delta\lambda$ of the Filters with the Best Reconstruction and Mean, Standard Deviation, Maximum and Minimum P_{rec}, and *RMSE* Values for the Studied Cases

	Simulation									
	With Lamp $Tc_1 = 2852$ K					With Lamp $Tc_2 = 3371$ K				
Parameters	2[a]	3	4	5	6	2[a]	3	4	5	6
$\Delta\lambda$	81	36	66	27	100	78	36	69	26	100
Mean P_{rec}	93.782	98.540	99.758	99.995	99.996	93.392	98.438	99.761	99.994	99.996
Standard deviation P_{rec}	10.279	2.504	0.571	0.009	0.009	11.311	2.663	0.564	0.009	0.009
Maximum P_{rec}	99.991	99.993	100	100	100	99.992	99.994	100	100	100
Minimum P_{rec}	62.826	90.959	97.461	99.956	99.960	58.719	90.416	97.514	99.956	99.950
Mean (RMSE*100)	6.126	3.061	1.185	0.220	0.139	6.194	3.156	1.179	0.228	0.141
Standard deviation (RMSE*100)	5.131	2.646	1.022	0.206	0.139	5.335	2.572	1.021	0.214	0.140
Maximum (RMSE*100)	21.567	9.816	5.276	0.763	0.577	22.725	10.126	5.277	0.823	0.574
Minimum (RMSE*100)	0.745	0.657	0.086	0.044	0.016	0.716	0.627	0.088	0.044	0.017

[a]Number of filters.

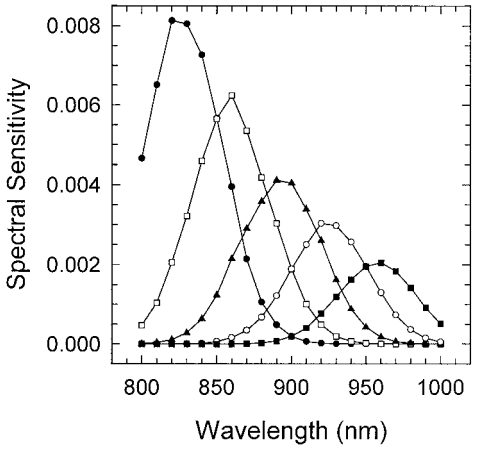

Fig. 10. Spectral sensitivity of the five optimum channels. The sensitivity includes the spectral response of the JAI CV-M10 camera, the emitted spectral radiance of the illuminant ($Tc_1 = 2852$ K), and the transmittance of the optimum filters.

Figure 12 shows the reconstruction parameters obtained with two and five filters for all the samples considered. It can be seen that when two filters are used, there are large errors in the results. With the use of five filters the dispersion of reconstruction parameters decreases and all the samples of the original data matrix have percentages of reconstruction similar to 100 and small (*RMSE**100) values. Two examples of reconstructed spectral reflectance with two and five filters are illustrated in Fig. 13. Meanwhile there are large differences between the original and the reconstructed spectra when two filters are used; the reconstructed spectra with five filters and the original spectra are almost the same.

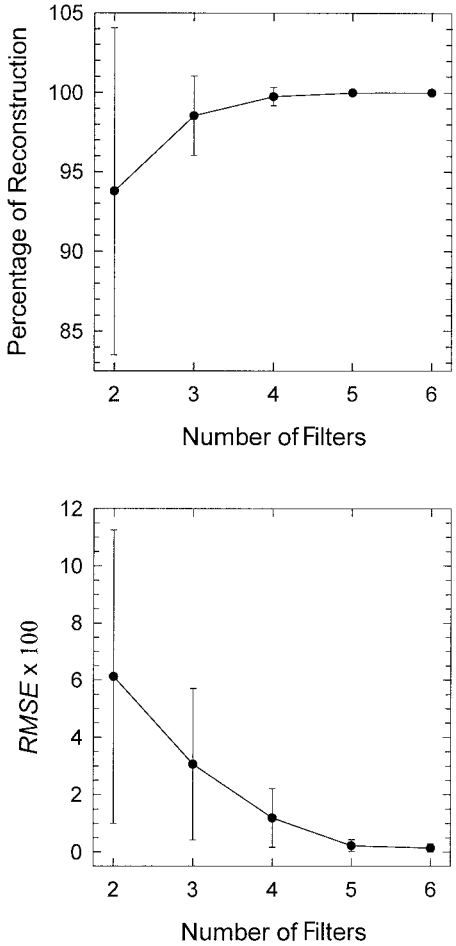

Fig. 11. Mean percentage of reconstruction and *RMSE* with the corresponding standard deviation for 2, 3, 4, 5, and 6 filters when the illuminant of color temperature, $Tc_1 = 2852$ K, is used.

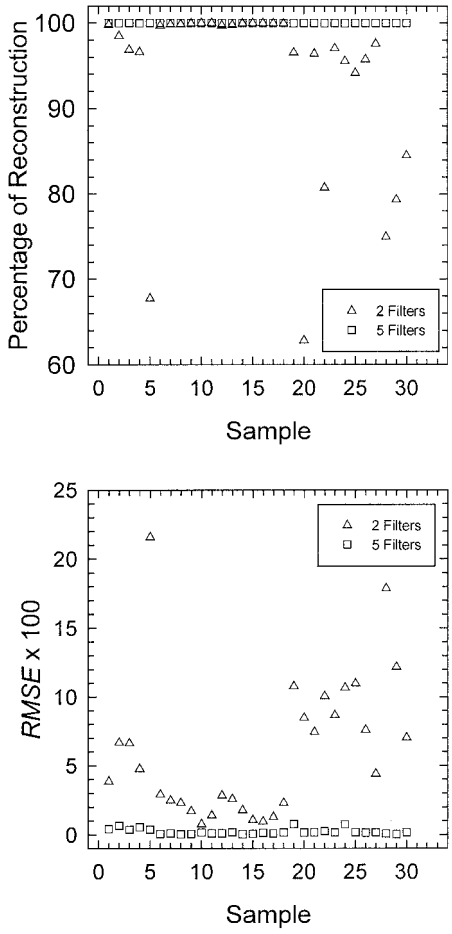

Fig. 12. Percentage of reconstruction and *RMSE* of the samples that belong to the original data matrix obtained with the illuminant of color temperature, $Tc_1 = 2852$ K, for 2 and 5 filters.

On the other hand, we noted that the results are fairly independent of the illuminant used. This low dependency may be due to the smoother spectral distribution of the radiance of the illuminant compared with the spectral sensitivity of the CCD camera. The reconstruction parameters have similar values in both cases, and the best filters are almost the same (the same value for parameter $\Delta\lambda$). This indicates that with the same set of filters we can obtain good reconstructions for every type of illuminant.

Finally, we performed another numerical simulation for different existing reconstruction methods to compare their ability. The tested methods were linear interpolation, cubic interpolation, spline in-

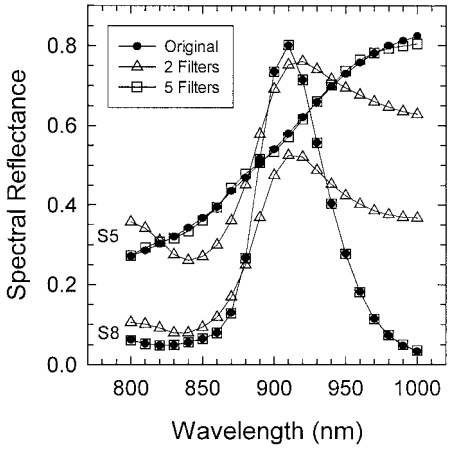

Fig. 13. Reconstructions of samples S5 and S8 of the original data matrix with 2 and 5 filters.

terpolation, the discrete Fourier-transform approximation, the modified discrete sine transform approximation, the Moore–Penrose pseudoinverse, the smoothing inverse, the Wiener inverse, and the nonlinear estimation (second-order polynomial). We used the same original data matrix, the illuminant of color temperature, $Tc_1 = 2852$ K, and the five optimum Gaussian filters obtained for each tested method. The mean percentage of reconstruction and *RMSE* for all the samples belonging to the original data matrix can be seen in Fig. 14. Almost all the existing reconstruction methods have poorer results than PCA except the Wiener inverse and the nonlinear estimation, which have very similar values of percentage of reconstruction and *RMSE* parameters.

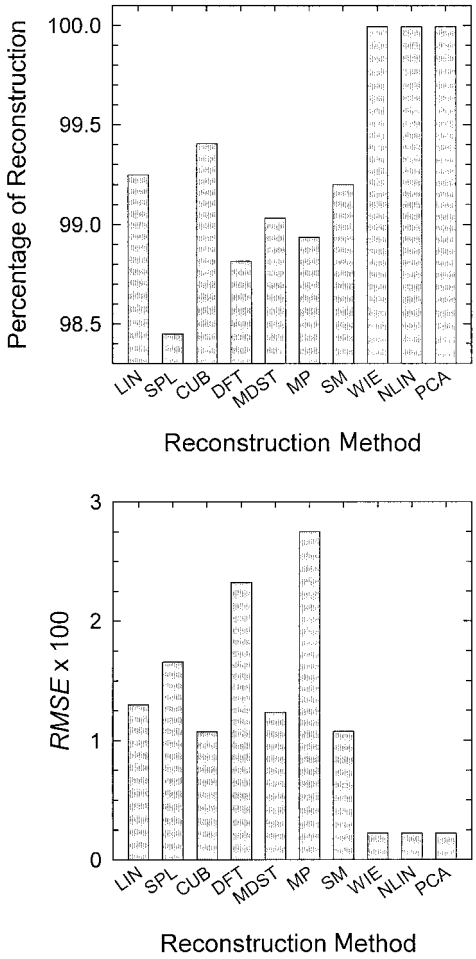

Fig. 14. Mean percentage of reconstruction and *RMSE* of the samples that belong to the original data matrix obtained for several existing reconstruction methods: LIN, linear interpolation; SPL, spline interpolation; CUB, cubic interpolation; DFT, discrete Fourier-transform approximation; MDST, modified discrete sine transform approximation; MP, Moore–Penrose pseudoinverse; SM, smoothing inverse; WIE, Wiener inverse; NLIN, nonlinear fitting; PCA. The illuminant of color temperature, $Tc_1 = 2852$ K, and the five optimum filters are used.

4. Conclusion

We have presented an experimental method for performing a spectral characterization for any digital image capture device (in our case a conventional CCD camera) in the NIR region. The profiles of the relative spectral responsivity (action spectrum) are independent of the exposure (normalized outputs). This feature allows the relative spectral sensitivity of the CCD camera to be calculated. The spectral sensitivity obtained for the camera is significant to as great as 1000 nm.

Using a PCA-based method, we have obtained the reconstruction of reflectance curves by analyzing multispectral images from a CCD conventional camera in the NIR region. Various filters need to be placed in front of the camera to obtain the acquisition channels. To determine the quality of the reconstructions and the number and shape of the filters that must be placed in front of the camera, we performed a numerical simulation. The parameters used to evaluate the reconstruction are the percentage of reconstruction and the *RMSE*. We analyzed the reconstructions obtained for 19 real samples and 11 theoretical samples, using 2–6 equispaced Gaussian filters under the influence of two different illuminants ($Tc_1 = 2852$ K and $Tc_2 = 3371$ K). The width of the Gaussian filters was optimized to obtain the best reconstruction parameters. According to the results, the reconstruction of the curves improves if the number of filters is increased. Using five filters, the reconstructed reflectance spectra are very similar to the original curves, and all the samples have percentages of reconstruction greater than 99.9% and (*RMSE**100) values smaller than one. With the use of more filters the reconstructions improve even more but the changes are not important. The shape of the optimum filters depends on the number of channels used, but in all the cases studied they have a large spectral width. Moreover parameter $\Delta\lambda$ is almost independent of the illuminant used, since this makes a smaller contribution than the spectral sensitivity of the CCD camera. This makes the method widely applicable, since the reconstructions may be performed in many lighting conditions when the same

set of filters is used. Therefore we have demonstrated that with a conventional CCD camera and five filters with a large spectral width, which therefore are commercially available, it is possible to obtain good spectral reflectance reconstructions in the NIR region.

This research was supported by the Comisión Interministerial de Ciencia y Tecnología (CICYT), Spain, under grant TAP-99-0856.

References

1. G. C. Holst, *CCD Arrays, Cameras and Displays* (SPIE Press, Bellingham, Wash., 1998).
2. G. C. Holst, "Solid-state cameras," in *Handbook of Optics*, Vol. 3, M. Bass, J. M. Enoch, E. W. Van Stryland, and W. L. Wolfe, eds. (McGraw-Hill, New York, 2001), pp. 4.1–4.21.
3. D. A. Burns and E. W. Ciurczak, *Handbook of Near-Infrared Analysis* (NIR Publications, Chichester, West Sussex, UK, 1999).
4. D. Scribner, P. Warren, and J. Schuler, "Extending color vision methods to bands beyond the visible," Mach. Vision Appl. **11,** 306–312 (2000).
5. D. Scribner, P. Warren, J. Schuler, M. Satyshur, and M. Kruer, "Infrared color vision: an approach to sensor fusion," Opt. Photon. News **9,** 27–32 (1998).
6. F. M. Martinez-Verdú, J. Pujol, and P. Capilla, "Calculation of the color matching functions of digital cameras from their complete spectral sensitivities," J. Imaging Sci. Technol. **46,** 15–25 (2002).
7. M. D. Mermelstein, K. A. Snail, and R. G. Priest, "Spectral and radiometric calibration of midwave and longwave infrared cameras," Opt. Eng. **39,** 347–352 (2000).
8. L. Poletto, A. Boscolo, and G. Tondello, "Characterization of a charge-coupled-device detector in the 1100–0.14-nm (1–9-keV) spectral region," Appl. Opt. **38,** 29–36 (1999).
9. The International Organization for Standarization (ISO), ISO/TC42 (Photography), WG18 (Electronic Still Picture Imaging), DIS-ISO 14524: Photography—electronic still picture cameras—methods for measuring opto-electronic conversion functions (OECFs) (ISO, Geneva, 1999).
10. L. W. MacDonald and W. Ji, "Color characterization of a high-resolution digital camera," in *Proceedings of the First European Conference on Color in Graphics, Imaging, and Vision* (CGIV 2002) [Society for Imaging Science and Technology (IS&T), 7003 Kilworth Lane, Springfield, Va. 22151, 2002], Vol. 1, pp. 433–437 (ISBN 0-89208-239-9).
11. J. Y. Hardeberg, H. Brettel, and F. Schmitt, "Spectral characterization of electronic cameras," in *Electronic Imaging: Processing, Printing and Publishing in Color*, J. Bares, ed., Proc. SPIE **3409,** 100–109 (1998).
12. P. M. Hubel, D. Sherman, and J. E. Farrell, "A comparison of methods of sensor spectral sensitivity estimation," in *Proceedings of the Second Color Imaging Conference: Color Science, Systems, and Applications* [The Society for Imaging Science and Technology (IS&T), 7003 Kilworth Lane, Springfield, Va. 22151, 1994], Vol. 48, pp. 45–48 (ISBN: 0-89208-180-5).
13. G. Hong, M. R. Luo, and P. Rhodes, "A study of digital camera colorimetric characterization based on polynomial modeling," Color Res. Appl. **26,** 76–84 (2001).
14. J. L. Simonds, "Application of characteristic vector analysis to photographic and optical response data," J. Opt. Soc. Am. **53,** 968–974 (1963).
15. F. Imai and R. S. Berns, "Comparative analysis of spectral reflectance reconstruction in various spaces using a trichromatic camera system," J. Imaging Sci. Technol. **44,** 280–287 (2000).
16. M. J. Vrhel, R. Gershon, and L. S. Iwan, "Measurement and analysis of object reflectance spectra," Color Res. Appl. **19,** 4–9 (1994).
17. M. J. Vrhel and H. J. Trussell, "Color correction using principal components," Color Res. Appl. **17,** 4–9 (1992).
18. J. Y. Hardeberg, F. Schmitt, H. Brettel, J. Crettez, and H. Maître, "Multispectral image acquisition and simulation of illuminant changes," in *Colour Imaging: Vision and Technology*, L. W. MacDonald and M. R. Luo, eds. (Wiley, Chichester, UK, 1999), pp. 145–164.
19. Y. Chang, P. Liang, and S. Hackwood, "Unified study of color sampling," Appl. Opt. **28,** 809–813 (1989).
20. F. König, "Reconstruction of natural spectra from a color sensor using nonlinear estimation methods," in *Proceedings of IS&T 50th Annual Conference* (Society for Imaging Science and Technology, Springfield, Va., 1997), pp. 454–458.
21. P. L. Vora and H. J. Trussell, "Mathematical methods for the design of color scanning filters," IEEE Trans. Image Process. **6,** 312–320 (1997).
22. P. L. Vora and H. J. Trussell, "Mathematical methods for the analysis of color scanning filters," IEEE Trans. Image Process. **6,** 321–327 (1997).
23. M. Wolski, C. A. Bouman, J. P. Allebach, and E. Walowit, "Optimization of sensor response functions for colorimetry of reflective and emissive objects," IEEE Trans. Image Process. **5,** 507–517 (1996).
24. M. J. Vrhel and H. J. Trussell, "Design and realization of optimal color filters for multiilluminant color correction," J. Electron. Imaging **4,** 6–14 (1995).
25. M. J. Vrhel and H. J. Trussell, "Filter considerations in color correction," IEEE Trans. Image Process. **3,** 147–161 (1994).
26. G. Sharma and H. J. Trussell, "Figures of merit for color scanners," IEEE Trans. Image Process. **6,** 990–1001 (1997).
27. P. L. Vora and H. J. Trussell, "Measure of goodness of a set of color-scanning filters," J. Opt. Soc. Am. A **10,** 1499–1508 (1993).
28. F. M. Martinez-Verdú, J. Pujol, A. Bouzada, and P. Capilla, "Spectroradiometric characterization of the spectral linearity of a conventional digital camera," in *Color Imaging: Device-Independent Color, Color Hardcopy, and Graphic Arts IV*, G. B. Beretta and R. Eschbach, eds., Proc. SPIE **3648,** 279–290 (1999).